Rheol Acta (2000) 39: 201–208

ORIGINAL CONTRIBUTION

Flow in micellar cubic crystals

Erika Eiser
François Molino
Grégoire Porte
Xavier Pithon

Received: 30 November 1999
Accepted: 30 November 1999

E. Eiser (✉)
European Synchrotron Radiation Facility
BP 220, F-38043 Grenoble, France
e-mail: eiser@esrf.fr

F. Molino · G. Porte · X. Pithon
Groupe de Dynamique des Phases
Condensées, Université de Montpellier II
F-34095 Montpellier Cedex 05, France

Presented at EuroRheo 99-1, May 3–7, 1999, Sophia-Antipolis, France

Abstract We investigate and compare the mechanical properties of two micellar cubic crystals. Both are obtained from aqueous triblock-copolymer solutions of similar block structure, $(PEO)_{76}(PPO)_{29}(PEO)_{76}$ and $(PEO)_{127}(PPO)_{48}(PEO)_{127}$, designated Pluronic F68 and F108 respectively. Extensive small angle X-ray scattering experiments under shear and common rheometry provide the following results: (i) the solid phases of the two polymeric solutions are constituted of micelles that are ordered in a bcc (F68) and fcc (F108) structure. The overall appearance of both unsheared samples is polycrystalline; (ii) SAXS showed that both systems undergo a structural reorientation under shear, with the dense planes arranged parallel to the velocity - vorticity plane, thus facilitating flow; (iii) F68 showed a clear transition in the flow curve, associated with a textural change, but the F108 system exhibited a continuous evolution; (iv) the bcc crystal appears to have no measurable yield stress and flows even for low applied stresses. This was in contrast to the fcc sample which showed a clear yield stress, separating creep and flow regimes.

Key words Micellar cubic phase · Shear-banded flow · Textural transition

Introduction

The study of the flow behaviour of cubic phases made of surfactants or copolymers has been for years an active part of the general problem of structural transitions under flow and of the correlation between these textural or phase transitions and the corresponding mechanical response (Ackerson et al. 1981; Chen et al. 1992, 1994; Buter et al. 1996; Diat et al. 1996; Lie et al. 1996a; Kleppinger et al. 1997; Hamley et al. 1998; Molino et al. 1998; Eiser et al. in print). Inspired by the work of Ackerson and Zukoski on charge stabilised colloids (Ackerson et al. 1981; Chen et al. 1992; Pusey et al. 1989), we investigated two systems of soft spheres arranged to obtain long-range crystalline order at a much lower space scale, based on the auto-aggregating properties of triblock copolymers.

Two aqueous systems of differently long polymers, $(PEO)_n(PPO)_m(PEO)_n$ (with n and m taking different values), were probed. The entire copolymer is very soluble at 5 °C, but the PPO part becomes hydrophobic at higher temperatures, leading to the creation of monodispersed micelles (Zhou and Chu 1994; Berret et al. 1996). At high enough concentrations, the constraints of space filling lead to a liquid-to-solid transition with long-range order. Although 'soft', the systems have elastic moduli higher than typical values for colloidal crystals, and far lower than conventional crystals. The typical mesh size, a, is between 70 Å and 300 Å (the elastic energy scales as $1/a^3$). Using conventional stress- or strain-controlled rheometers, these materials can be easily submitted to deformations leading to flow. Behaviour of shear alignment, fracture, and creep have been investigated for different values of the applied stress or shear rate. Our goal here is to present and to compare qualitatively the results for flow behaviour of two systems, having different local symmetries. Namely, the micelles of the polymer, F108

($n = 127$, $m = 48$), organise themselves into face-centred cubic (*fcc*) symmetry, and the $n = 76$, $m = 29$ system (F68) leads to a body-centred cubic (*bcc*) symmetry. In order to understand the findings for the mechanical behaviour of such crystalline structures we will first present a brief summery of small-angle X-ray data obtained for the same samples under shear.

Experimental

We used two symmetric triblock copolymers, polyethylene oxide – polypropylene oxide – polyethylene oxide $(PEO)_{76}(PPO)_{29}(PEO)_{76}$ and $(PEO)_{127}(PPO)_{48}(PEO)_{127}$, commercially known as F68 and F108 respectively. These co-polymers were purchased from SERVA (Germany) and used as received without further purification. All samples were prepared with water, purified using a Millipore filtration unit.

46 wt% solutions of F68 and 35 wt% solutions of F108 are prepared by dissolving the polymer in water at low temperature ($T = 5$ °C), where water is a good solvent for both the PEO and PPO parts. As the solubility of PPO in water decreases on reaching room temperature, micelles are formed by spontaneous association and for the concentrations mentioned above, a liquid-to-solid transition is observed (Zhou and Chu 1994). We use 23 °C for F68 and 25 °C for the F108 solutions as working temperatures as these are well within the solid phase.

Rheology experiments were performed using a stress-controlled rheometer in a Couette (Physica USD 200; the diameter of the rotating inner bob is 12.5 mm and the gap width 1.06 mm) and a cone-plate geometry (the diameter of the cone was 50 mm, with an angle of 1°). The liquid solution was inserted into the pre-cooled cell and, after immersing the rotor into the sample, heated to the temperatures given above in order to avoid any pre-shear of the sample. At the liquid-to-solid transition a strong pulling force was observed, hence the sample was left to relax for two hours prior to any experiment.

All SAXS experiments were performed at the ESRF-Grenoble (beam line ID2), using a rate-controlled Couette cell with an outer cylinder/gap ratio of 20/1mm. The X-ray wave length used was 1 Å, with a resolution $\Delta\lambda/\lambda = 0.01$, and a sample to detector distance of 4 m. Diffraction patterns presented here were taken after cessation of shear, as strong continuous shear leads to destruction of the sample. Comparisons of X-ray images taken under shear and those taken at rest right afterwards verify the integrity of the procedure (for more details see Molino et al. 1998).

The setup of the Couette cell allows for the exploration of two geometries: 1) radial, where the X-ray impinges on the sample perpendicularly to the velocity and the vorticity 2) tangential (not shown here), where the beam is parallel to the velocity vector and perpendicular to the vorticity. In addition, the narrow width of the beam (~150 μN) allows scanning of the 1mm broad gap which enables a spatial analysis of the probe.

Results and discussion

Structure before and after shear

In this chapter we give a brief overview of the structural analysis of the two cubic symmetries, obtained from small-angle X-ray scattering under shear. As a result we will be able to understand and interpret the rheological behaviour of the samples, the main point of interest in the present work. Thus the reader may find a detailed SAXS analysis in the references (Molino et al. 1998; Eiser et al. in print).

Small-angle X-ray diffraction performed on F68 and F108 samples, crystallised in situ, show powder diffraction rings which can be identified with a local cubic structure, while the overall image is that of a "grainy" powder-crystalline sample (Mc Connell et al. 1993; Molino et al. 1998). The micelles formed from F68 triblock copolymers have an aggregation number of about 7 and form a bcc powder-crystal with a lattice size of 100 Å, and a nearest-neighbour distance of around 74 Å. However, F108 micelles, which have a thicker hydrated corona, crystallise into an fcc phase (the aggregation number is around 50). Here the lattice parameter is 294 Å, and the separation between nearest neighbours is 208 Å. Although the ratio of the PPE to PPO block is similar in both polymers, one forms an *fcc* and the other a *bcc* structure. This implies that the interaction potential of the F108 micelles is different from the F68 micelles. Regarding the greatly different aggregation number, one sees that a considerably smaller number of PPE arms constitute the corona of the F68 micelles. A less dense corona, however, suggests that the interaction potential will not be the one of a truly hard sphere but the one with an additional long-range repulsion as proposed by McConnell et al. 1993. Spheres with such an extended interaction potential are expected to form less dense orders. In view of this F108 micelles, which have a much denser corona and thus approach the hard-sphere situation, crystallize into the close packing *fcc* structure.

Once shear is applied to the samples, a transition from a powder-crystalline to a highly aligned sample is observed (McConnell et al. 1993; Molino et al. 1998). Figure 1 presents the radial view of a F68 sample (46 wt% at $T = 20$ °C) previously sheared at 356 s^{-1}. The sharp diffraction peaks reveal a strong homogeneous orientation of *bcc* structure, with the dense direction [1 1 1] parallel to the velocity, v, and the dense plane (1 1 0) parallel to the shear plane. Moreover the symmetry indicates that the two twins are present in equal proportions, thus we are not dealing with a single crystal (note that the boundary between the twins lies in the direction of the velocity). At these high shear rates flow is thus facilitated by the reorientation of the dense planes parallel to the walls of the Couette cell so that they can slide past each other.

Similar reorientation or layer-sliding structure is observed in the *fcc* sample (35 wt% solution at 25 °C, after a pre-shear rate of 300 s^{-1}), as presented by the radial view in Fig. 2. The six intense Bragg-peaks stem from the 2d hexagonal close packed (hcp) layers, aligned parallel to the Couette walls. The more faint inner dots are related to the stacking faults between the *hcp*-layers. Indeed the tangential view (not shown here) reveals that

the correlation, …ABCABC…, typical for *fcc* crystals is lost (Molino et al. 1998).

The objective of this work is to relate the structural changes of soft cubic crystals under shear with their macroscopic mechanical behaviour. Thus we present in the following paragraph the rheological measures obtained starting from the polycrystalline and layer-sliding regime.

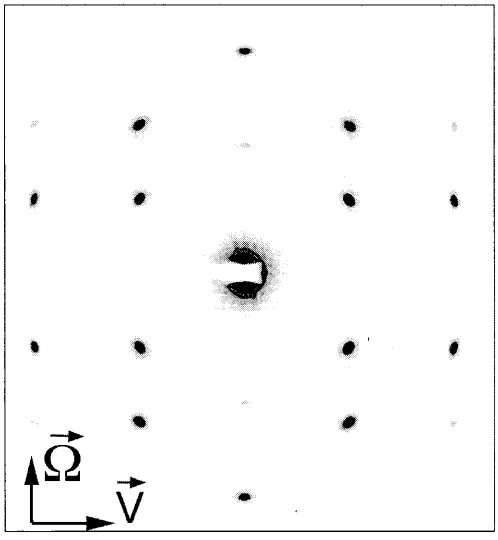

Fig. 1 Small angle X-ray diffraction pattern of a 46 wt% F68 (*bcc*) sample at $T = 20$ °C, measured in radial geometry. The sample was pre-sheared at $\dot{\gamma} = 365\ s^{-1}$. The symmetry of the 4 diffraction spots on the fist-order ring reflects the presence of a twin structure

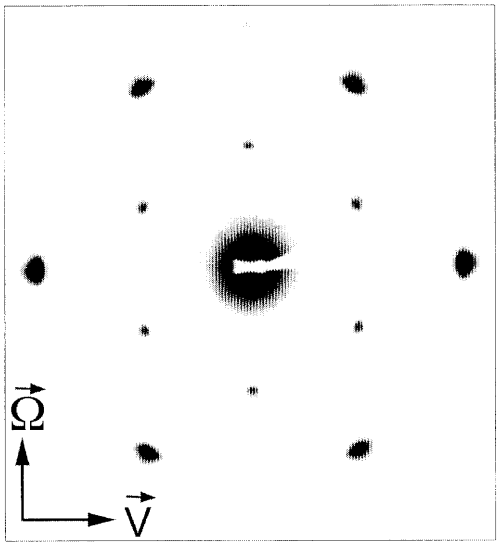

Fig. 2 SAXS image taken from a 35 wt% F108 (*fcc*) sample at $T = 25$ °C, in radial geometry. The sample was pre-sheared at $\dot{\gamma} = 200\ s^{-1}$. The intense diffraction spots correspond to the second order structure factor of 2d *hcp* planes which are perpendicular to the incoming X-rays and parallel to the shear plane. The faint inner spots stem from the piling up of stacking faults between the *hcp* planes

Flow-curve and the corresponding textural transitions

In Figs. 3 and 4 we present the flow-curves of both the *bcc* and *fcc* samples (Eiser et al. in print). Firstly we discuss the flow behaviour of the F68 sample. Using a cone-plate geometry, a continuously increasing stress (of step rate $\Delta\sigma = 1$ Pa) is applied to the initially polycrystalline sample and the corresponding shear rate is measured. Above a certain stress a sharp plateau occurs where, for a small change in σ, the shear rate jumps from around 6 s^{-1} to 40 s^{-1}, followed by a slow increase in $\dot{\gamma}$. Finally, with further increasing stress a second jump occurs from $\dot{\gamma} = 130\ s^{-1}$ to 400 s^{-1}. Repeated experiments show that the two plateaux always occur in the same shear-rate range, while the stress value for the first plateau varies strongly, depending on the contribution from the borders of the cone (which cannot be controlled). These two plateaux are correlated with the existence of three different stable states of the sample: a polycrystalline state, prevalent below 6 s^{-1}; a highly ordered state with the dense planes parallel to the shear plane, above $\dot{\gamma} \approx 130\ s^{-1}$; from detailed analysis of tangential X-ray diffraction patterns of samples sheared at $\dot{\gamma} \approx 50\ s^{-1}$, a third state, the texture of which is found to be of the same highly ordered *bcc* structure but with the dense planes perpendicular to the shear plane (Eiser et al. in print). To summarise, rheology experiments distinguish three distinct regimes of flow, ruled by the prevalent shear rate. Each of the flow regimes is characterised by the appearance of a new texture. From a polycrystalline texture at low shear rates, we come across two highly ordered textures which differ from one

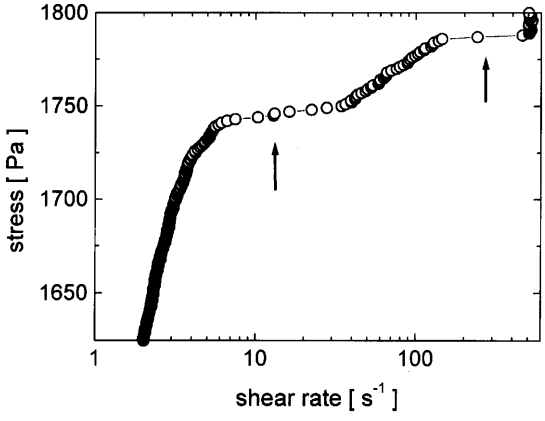

Fig. 3 Flow-curve of a 46 wt% F68 (*bcc*) sample measured in cone-plate geometry at $T = 20$ °C: stress is applied in steps of 1 Pa to the initially polycrystalline sample. The two arrows indicate the two plateau regions

another only by the spatial orientation of the dense planes. One can speak of an alignment transition since all three different textures exhibit local *bcc* structure with the same lattice size. In addition the textural transitions are reversible (not shown here): though the flow-curve shows strong hysteresis on decreasing stress the same stress plateaux are found in a second measure cycle. Also X-ray experiments show that a powder-crystalline texture is found again after shearing a highly oriented sample at low shear rates.

The flow behaviour of the *fcc* F108 sample is rather different from that of the one formed by F68; no plateau region is observed which could be related to a transition from the polycrystalline to layer-sliding texture. Data presented in Fig. 4 are measured in Couette geometry (cone-plate geometry provides similar results but is avoided because the Couette geometry reduces drying effects during long measurements). Returning to X-ray experiments we noticed that for a large range of shear rates, $0.1\ s^{-1} < \dot{\gamma} < 100\ s^{-1}$, a mixture of the powder crystalline and layer-sliding signature is present with a ratio of intensities dependent on the actual shear rate (Molino et al. 1998). This fraction of the layer-sliding phase increases with increasing shear rate and pervades the entire sample only at $\dot{\gamma} \approx 200\ s^{-1}$. As for the *bcc* sample, the polycrystalline texture is regained when the highly oriented sample is sheared at low shear rates for a couple of minutes. In spite of these structural similarities with the *bcc* crystal, two strikingly different features appear in the flow curve: the existence of a yield stress for the *fcc*; and the absence of a plateau in stress associated with the structural transition. The *fcc* system exhibits only strong shear thinning. Notice that below 300 Pa, no stationary flow can be achieved when starting from the polycrystal. On the other hand if one first strongly pre-shears and aligns the system first, and then decreases the stress, steady state flow can be achieved down to 160 Pa. We will come back to this dependence of the flow behaviour on the samples' initial condition later. The examination of the transient behaviour of the two systems under constant stress is necessary to obtain further indications.

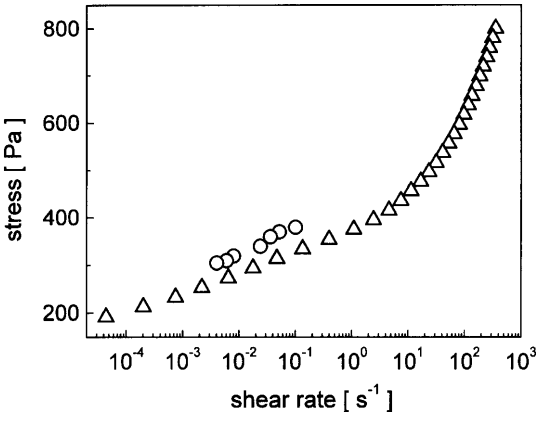

Fig. 4 Flow-curve of a 35 wt% F108 (*fcc*) sample measured in Couette geometry at $T = 25$ °C. The circles are measured in single long-time creep experiments starting out from polycrystalline samples (e.g. the data point for $\sigma = 310$ Pa was obtained from the creep curve shown in Fig. 5). The triangles are for the fully aligned sample, measured by descending the applied stress step wise (each point is measured for 2 mins, which appears to be sufficient to reach steady state)

Transient behaviour under stress

We show in Figs. 5 and 6 typical transient behaviour of the *fcc* and *bcc* systems respectively, exposed to small stresses, in the range of 1–100 Pa (Eiser et al. in print). For such small values, the *fcc* polycrystalline phase never reaches a steady state of constant shear rate. Instead we have creep behaviour of constant slowing down (see inset of Fig. 5), reminiscent of the one observed in metals. Above 300 Pa a new behaviour appears: after a long waiting time (which diverges as the stress decreases towards this 300 Pa), the viscosity of the sample drops by three orders of magnitude and the system begins to flow. The arrow in Fig. 5 indicates this turning point (circles presented in Fig. 4 were obtained from the slope of the flowing part in these long-time experiments). Such behaviour has been interpreted in terms of the nucleation of aligned lubricating bands of *hcp* layers, necessary to induce flow – in contrast to the much slower creep

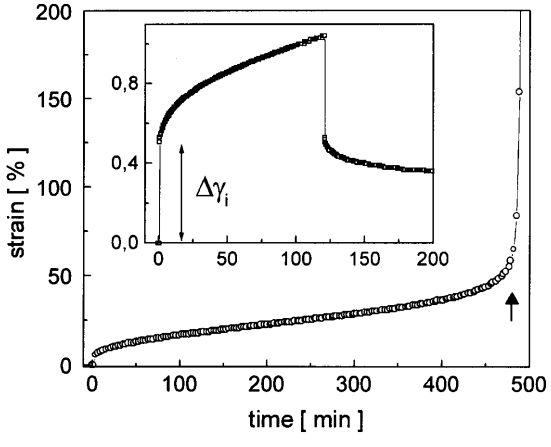

Fig. 5 Creep curve of a 35 wt% F108 (*fcc*) sample measured in Couette geometry at $T = 25$ °C. The applied stress is 310 Pa. The initial response is quite reminiscent of the *bcc* behaviour, except that no stationary state of flow (characterised by a constant slope) is reached in 3×10^4 s. After this time, the system begins to flow, with a sudden decrease in the viscosity by three orders of magnitude as indicated by the arrow (from 10^7 to 10^4 Pas). The inset shows a typical creep curve, here for an applied stress of 100 Pa, below the yield stress of the sample. Both curves were obtained starting out from a polycrystalline state

behaviour, associated with the reorganisation of grain boundaries. In other words, no flow behaviour is observed in absence of the layer-sliding phase. With X-rays we do not observe the aligned bands for small values of the shear rate, which is due to their small volume fraction up to 0.3 s^{-1}. This also explains the absence of any plateau in the flow curve: there are just no steady-state points below the stress corresponding to the nucleation of the aligned bands. In contrast, the F68 phase exhibits no, for us measurable, yield stress as the sample can flow with a constant rate even below 10 Pa (see Fig. 6). The associated shear rates are exceedingly small, and have been obtained from the time dependence of the deformation measured for around 10^3 seconds. Moreover, the typical decrease by three orders of magnitude in the apparent viscosity associated with the onset of flow in F108 has no equivalent in the F68 system. The small stress values of the shear rate continuously increase up to the stress plateau described previously. In fact the viscoelastic behaviour of the F68 phase can be accounted for by a quite simple superposition of a Maxwell and a Kelvin-Voigt element.

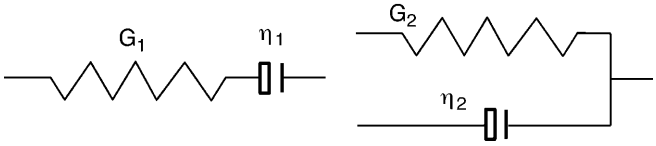

Multi-lamellar (onion) phases stacked in cubic order and exhibiting similar creep behaviour have been described using this simple model (Panizza et al. 1996). The instantaneous elasticity is accounted for by the G_1 modulus, the long time flow of the crystallites is described by the viscosity η_1. The Voigt modulus could describe the retarded elasticity associated with the dissipative displacement and growth of dislocation loops. Suitable values of the two time constants of the Maxwell and Voigt moduli enable one to reproduce the creep behaviour. Clearly this model cannot be used the plateau region in the *bcc* phase has been reached, where structural changes in the material are induced by the flow. For the *fcc* phase its validity is restricted to the range below the yield stress.

We offer no explanation for the difference in terms of steady-state behaviour under small stresses for the two phases. We can only tentatively conclude that the movement of defects in the grain boundaries is restricted in the *fcc* phase by the close-packed nature of the symmetry.

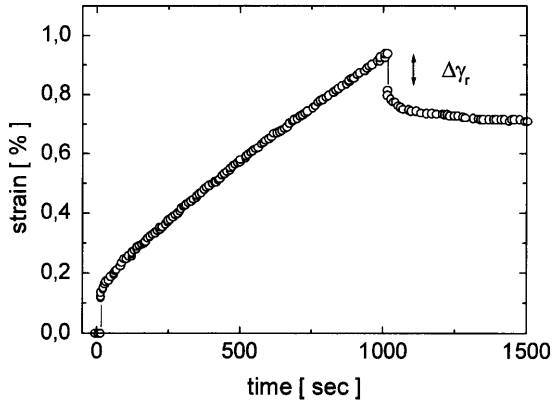

Fig. 6 Creep curve of a 46 wt% F68 (*bcc*) sample measured in Couette geometry at $T = 17$ °C. The applied stress is 50 Pa. A fast elastic response is followed by a non-stationary transient creep, leading to a stationary flow at long times

Elastic behaviour in the linear regime

Elastic moduli

As previously described, the creep behaviour of both materials is characterised by an instantaneous elastic response, $\Delta\gamma_i$, roughly equal to the instantaneous recoil, $\Delta\gamma_i$, observed immediately after relaxation of the force

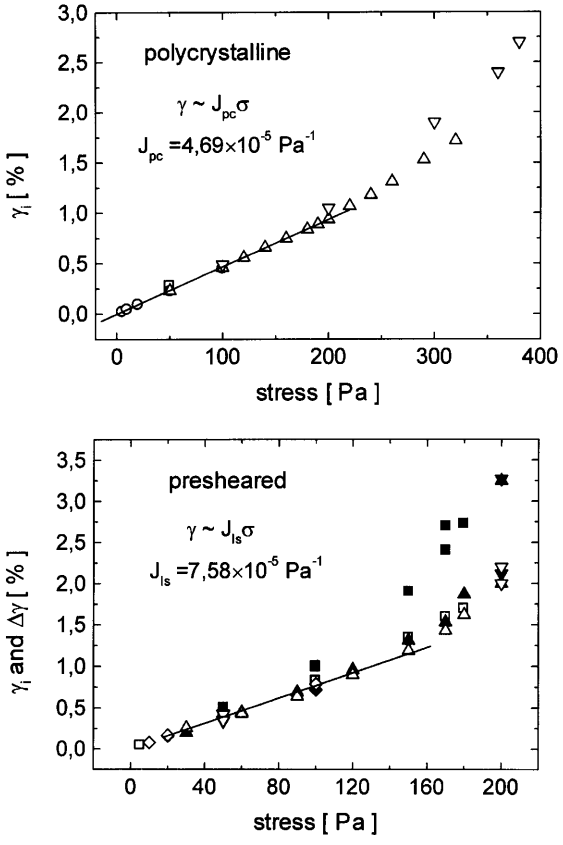

Fig. 7 Instantaneous elastic response, $\Delta\gamma_i$, of the F108 (*fcc*) phase, both in the polycrystalline and the pre-sheared (or aligned) state. The inverse of the creep compliance gives the elastic modulus: 20,000 Pa and 13,000 Pa respectively. Different symbols indicate in both figures different experimental series

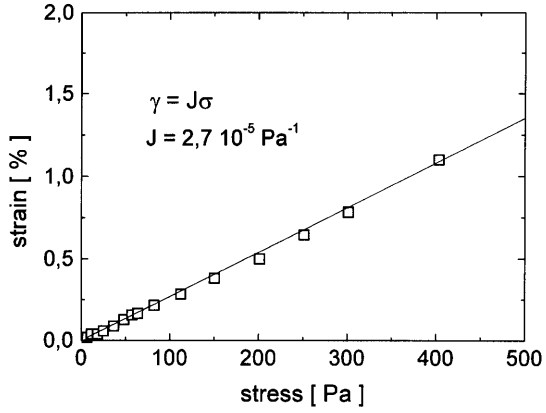

Fig. 8 Instantaneous elastic response of the F68 phase (*bcc*) in the polycrystalline state. The elastic modulus is around 40,000 Pa, twice the value of the *fcc* case

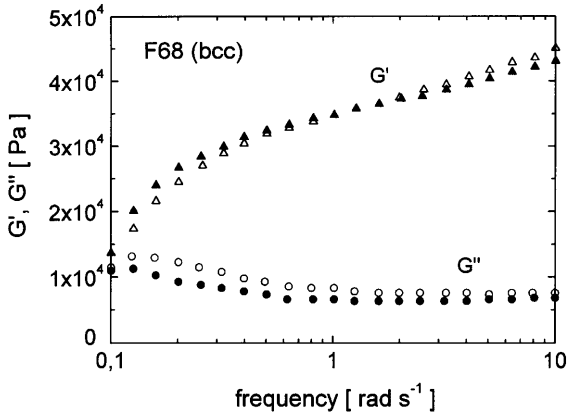

Fig. 9 Frequency dependence of the storage (triangles) and loss circles moduli for a F68 *bcc* sample in the polycrystalline (pre-shear at 0.1 s^{-1} open symbols) and aligned (pre-shear 150 s^{-1} closed symbols) configuration

(inset of Fig. 5). From the dependence on the applied stress of this elastic deformation, one can infer the value of the elastic modulus. We show in Figs. 7 and 8 the curves $\Delta\gamma_i(\sigma)$, for F108 both in the polycrystalline and pre-sheared (or aligned) state and for F68 in the polycrystalline state respectively. The elastic moduli (which is the inverse of the slope of $\Delta\gamma_i(\sigma)$, or compliance) vary for the F108 between 13,000 Pa (aligned sample) and 20,000 Pa (polycrystal), and is 41,000 Pa for the F68.

The elastic energy instantaneously stored (and as quickly released) in both systems is expected to be related to the elastic response of the ordered structure. However, the elastic modulus of the polycrystalline sample is almost twice of the pre-sheared one. This difference may be understood when considering the energy necessary for one dense plane to glide past the other. In the aligned state, the hexagonal close packed layers, *hcp*, are randomly stacked and lie in the shear plane. Similar to the *fcc* crystal, where the dense planes are perpendicular to the room diagonal $\langle 111 \rangle$, the *hcp* layers are separated by the distance $(3/4)^{1/2}a$. From the theory of dislocations in metallic crystals it is known that the energy corresponding to a displacement of a dislocation is proportional to the square of the Burgers vector, $E \propto b^2$, where b in our case can be related to the interplanar distance (West 1984). In a polycrystalline sample this cost in energy will be higher since one has to sum over all possible projections of Burgers vectors perpendicular to the shear plane, which are larger than $(3/4)^{1/2}a$. Thus, the applied stress in the shear-aligned sample can be more easily relaxed and it starts to flow earlier, while the polycrystal stores more stress elastically before succumbing to plastic deformation.

Furthermore, the mesh sizes of the F68 and F108 are 300 and 100 Å, respectively. Therefore we expect the ratio between the elastic moduli to be around 3^3, provided that the elastic energy scales as k_BT/a^3 (a being the typical lattice size, and which is three times smaller in the F68 *bcc)*. This simple scaling assumption clearly overestimates here the importance here of the mesh size difference. Moreover the details of the interaction potential play a crucial part in determining the modulus, which is in a simple periodic-potential picture just the curvature of the potential at the minimum. Here, this potential depends on details of the interaction between two coronas of PEO chains in good solvent. The differences in the radii of the hydrophobic cores and in the length of the side chains are difficult to take into account in such a simple picture.

Linear viscoelastic behaviour

The frequency dependence of the storage and loss moduli in the linear regime, both for pre-sheared and polycrystalline samples, have been measured for the two cubic phases. Care was taken to ensure that the dynamic measurements were performed in the linear regime, which lies for both crystals within 1% of deformation. Results are presented in Figs. 9 and 10. In both systems, we observe a weak influence of the pre-shear, and thus of the state of alignment, on the storage modulus, G', which is expected if the elasticity is associated with the unchanged local long-range order. The loss modulus, G'', is also weakly affected, and exhibits an increase for the small values of the frequency. This has been associated with a so-called 'soft glassy behaviour' (Mason and Weitz 1995; Liu et al. 1996b; Mason et al. 1996; Panizza et al. 1996; Mason and Bibette 1997; Sollich et al. 1997; Buzza et al. 1995; Hébraud et al. 1997), and the existence of a range of very long relaxation times (around 100 s here). This is consistent with the creep behaviour in *fcc* samples, where the system reaches the flow regime only after a long

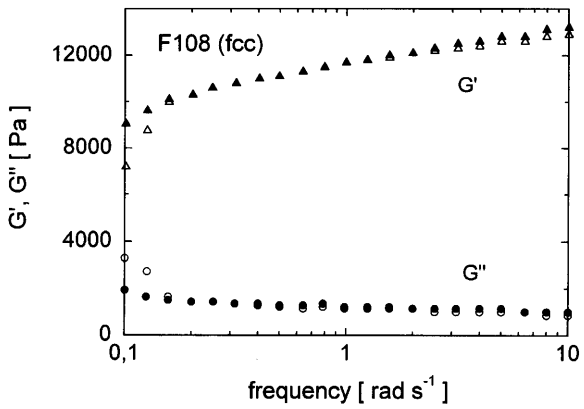

Fig. 10 Frequency dependence of the storage (triangles) and loss circles moduli for a F108 *fcc* sample in the polycrystalline (pre-shear at 0.1 s^{-1} open symbols) and aligned (pre-shear 150 s^{-1} closed symbols) configuration

transient. As expected it is difficult to predict from our data the value for which $G''(\omega)$ reaches a maximum before going down to zero at even lower frequencies. The upper limit of the range of relaxation times present in the system, which should be accounted for by several Kelvin-Voigt moduli in our simple picture, is thus undetermined. Hence the 'glassy' character of the material remains uncertain.

Conclusions

To conclude we summarize the features of our system that we have qualitatively discussed. First, the correlation between the structural evolution (alignment) and the mechanical signature under flow (strong shear thinning or plateau), in both the F68 and the F108, exemplifies on a new system the well studied behaviour of shear induced transitions. Although the case of the *fcc* seems less clear, due to the decorrelation between the aligned layers, it seems appropriate to renounce the 'phase transition under shear' vocabulary, as used for example in the case of giant micelles, and to speak rather of textural transitions due to the flow. The second (and related) aspect of our systems, which should be worth further inquiry, is the creep behaviour, and the analogy with polycrystalline metals under load. We have developed in another paper (Eiser, Molino and Porte in print) the analogy between the nucleation of the fluid aligned layers and the growth of a fracture in metallic alloys that the similarity of the creep behaviours suggests. This view of the nucleation of a far less viscous band as a fracture is certainly an insight which could be helpful in the other materials exhibiting shear banding and shear thinning.

In the polycrystalline state, these system seems to be particularly suitable to the study of quenched disorder, and a deeper understanding of the dependence on the grain sizes, temperature of quench, and local symmetry, is still missing. We expect the general perspective of the 'soft glassy materials' models to give a suitable background to this investigation.

Acknowledgements We want to thank the European Community, which supported this work through the TMR network (contract ERBFMRX-CT96-0003). We would also like to thank Olivier Diat who helped us with the SAXS-experiments at the ESRF.

References

Ackerson BJ, Clark NA (1981) Shear-Induced Melting. Phys Rev Let 46(2):123–126

Berret JF, Molino F, Porte G, Diat O, Lindner P (1996) The shear-induced transition between oriented textures and layer-sliding-mediated flows in a micellar cubic crystal. J Phys Condens Matter 8:9531–9517

Butera RJ, Wolfe MS, Bender J, Wagner NJ (1996) Formation of a highly ordered colloidal microstructure upon flow from high shear rates. Phys Rev Lett 77(10):2117–2120

Buzza DMA, Lu CYD, Cates ME (1995) Linear shear rheology of incompressible foams. J Phys II France 5:37–52

Chen LB, Zukoski CF, Ackerson BJ, Hanley HJM, Straty GC, Barker J, Glinka CJ (1992) Structural changes and orientational order in a sheared colloidal suspension. Phys Rev Lett 69(4):688–691

Chen LB, Chow MK, Ackerson BJ, Hanley HJM, Straty GC, Barker J, Glinka CJ (1994) Rheological and microstructural transitions in colloidal crystals. Langmuir 10:2817–2829

Diat O, Porte G, Berret JF (1996) Orientation and twins separation in a micellar cubic crystal under oscillatory shear. Phys Rev B 54(21):14 869–14 872

Eiser E, Molino F, Porte G (in print) Correlation between the viscoelastic properties of a soft crystal and its microstrcture. EPJE

Eiser E, Molino F, Porte G, Diat O (in print) Non-homogeneous textures and banded flow in a soft cubic phase under shear. Phys Rev E

Hamley IW, Pople JA, Fairclough JAP, Ryan AJ, Booth C, Yang YW (1998) Shear-induced orientational transitions in the body-centred cubic phase of a diblock copolymer gel. Macromolecules 31(12):3906–3911

Hébraud P, Lequeux F, Munch JP, Pine DJ (1997) Yielding and rearrangements in disordered emulsions. Phys Rev Lett 78(24):4657–4660

Kleppinger R, Mischenko N, Theunissen E, Reynaers HL, Koch MHJ, Almdal K, Mortensen K (1997) Shear-induced single crystalline mesophases in physical networks of gel-forming triblock copolymer solutions. Macromolecules 30:7012–7014

Liu YC, Chen SH, Huang JS (1996a) Relationship between the microstructure and rheology of micellar solutions formed by a triblock copolymer surfactant. Phys Rev E 54(2):1698–1708

Liu AJ, Ramaswamy S, Mason TG, Gang H, Weitz DA (1996b) Anomalous viscous loss in emulsions. Phys Rev Lett 76(16):3017–3020

Mason TG, Weitz DA (1995) Linear viscoelasticity of colloidal hard sphere suspensions near the glass transition. Phys Rev Lett 75(14):2770–2773

Mason TG, Bibette J, Weitz DA (1996) Yielding and flow of monodisperse emulsions. J Colloid Interface Sci 179:439–448

Mason TG, Bibette J (1997) Shear rupturing of droplets in complex fluids. Langmuir 13(17):4600–4613

McConnell GA, Gast AP, Huang JS, Smith SD (1993) Disorder-order transition in soft sphere polymer micelles. Phys Rev Lett 71(13):2102–2105

Molino FR, Berret JF, Porte G, Diat O (1998) Identification of flow mechanisms for a soft crystal. Eur Phys J B 3:59–72

Panizza P, Roux D, Vuillaume V, Lu CYD, Cates ME (1996) Viscoelasticity of the onion phase. Langmuir 12:248–252

Pusey PN, van Megen W, Bartlett P, Ackerson BJ, Rarity JG, Underwood SM (1989) Structure of crystals of hard colloidal spheres. Phys Rev Lett 63(25):2753–2756

Sollich P, Lequeux F, Hébraud P, Cates MC (1997) Rheology of soft glassy materials. Phys Rev Lett 78:2020

Zhou Z, Chu B (1994) Phase behaviour and association properties of poly(oxypropylene) – poly(oxyethylene) – poly(oxypropylene) triblock copolymer in aqueous solution. Macromolecules 27:2025–2033

West AR (1984) Solid state chemistry and its applications. Wiley, New York